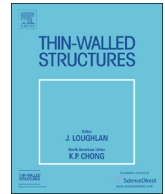




Contents lists available at ScienceDirect

Thin-Walled Structures

journal homepage: [www.elsevier.com/locate/tws](http://www.elsevier.com/locate/tws)

Full length article

## Behavior of single-box multi-cell box-girders with corrugated steel webs under pure torsion. Part I: Experimental and numerical studies

Kongjian Shen<sup>a</sup>, Shui Wan<sup>a,\*</sup>, Y.L. Mo<sup>b</sup>, Aiming Song<sup>a</sup>, Xiayuan Li<sup>a</sup><sup>a</sup> School of Transportation, Southeast University, Nanjing 210096, China<sup>b</sup> Department of Civil and Environmental Engineering, University of Houston, Houston 77204, USA

## ARTICLE INFO

## Keywords:

Single-box multi-cell box-girder  
Corrugated steel web  
Pure torsional test  
Finite element analysis  
Torque-twist curve  
Shear strain

## ABSTRACT

This paper presents the experimental and numerical studies on the full torsional behavior of single-box multi-cell box-girders with corrugated steel webs (BGCSWs) under pure torsion. Two specimens of BGCSWs with double cells and triple cells are tested under pure torsion using a new apparatus. Then the accuracy and efficiency of finite element analysis (FEA) models are validated by comparing with the experimental results, including the overall torque-twist curves, crack patterns of concrete slabs and shear strains in concrete slabs and corrugated steel webs (CSWs). Next, a parametric study is carried out, which shows that the torsional capacity is in linear proportion to the compressive strength of concrete, the thickness, yield strength and transverse position of CSWs and the number of cells in the given ranges. Besides, this study demonstrates that the CSW located at the torsional center of multi-cell BGCSWs has little effect on the torsional responses and the other inner CSWs in the multi-cell BGCSWs have little contribution to the cracking torques but have significant effects on the yield and ultimate torques. At last, a new fitted formula for the relations of smeared shear strains between the inner CSWs and the outermost CSWs is obtained from a series of case studies.

## 1. Introduction

The box-girders with corrugated steel webs (BGCSWs) have been widely used in bridge construction around the world since the first prestressed concrete box-girder bridge with corrugated steel webs (CSWs), Cognac Bridge, emerged in France in 1986 [1]. Especially in Japan and China, the overall numbers of newly built or under construction bridges using BGCSWs have exceeded 200 and 60 [2,3], respectively. The widespread usage of this kind of steel-concrete composite structures can be attributed to their remarkable advantages such as significantly reducing the structural self-weight, accelerating the construction speed, improving the efficiency of prestressing, completely avoiding the problem of web cracking, and so on [4,5]. Most of the prestressed concrete box-girder bridges with CSWs were designed as single-cell BGCSWs for the past three decades, especially in Japan [2]. However, with the rapid increasing of traffic flow, such as in China, the wide multi-cell BGCSWs are gradually applied in the highway and municipal bridges to provide more traffic lanes. This requires more researches on the behavior of this type of structure. Through intensive literature investigation, it can be found that many valuable investigations have been conducted on the flexural [6–11] and shear [12–14] behaviors of BGCSWs, and few studies have focused on the torsional

behavior of BGCSWs, especially that of multi-cell BGCSWs. However, the replacement of traditional flat concrete webs by CSWs will make the torsional stiffness of the structure to be the 30–40% of that of conventional concrete box-girder [15]. In addition, torsion can be regarded as a primary effect in some special cases, such as curved girders and eccentrically loaded girders, especially the torsional responses of wide multi-cell BGCSWs are more prominent under large eccentric load. Hence, it is of great importance to perform detailed researches on the torsional behavior of multi-cell BGCSWs.

The current investigation methods on the torsional behavior of BGCSWs includes experimental, numerical and theoretical analyses. The recent progress in theoretical analysis will be presented in the companion paper [16]. According to the different stages of loading, the experimental and numerical analyses can be divided into two categories: linear elastic analysis and plastic limit analysis. Most investigators have focused their experimental and numerical studies on the elastic torsional responses of BGCSWs under eccentric load, which is closest to the true loading state. The studies under this loading condition mainly included structural responses of torsion and distortion [17–21], transverse internal forces [22,23], transverse distribution coefficient of applied load [24], eccentric load coefficient [25] and torsional vibration characteristic [26,27]. Some investigators have

\* Correspondence to: School of Transportation, Southeast University, Nanjing 210096, Jiangsu, China.

E-mail addresses: [aimingskj@gmail.com](mailto:aimingskj@gmail.com) (K. Shen), [lanyu421@163.com](mailto:lanyu421@163.com) (S. Wan), [yilungmo@central.uh.edu](mailto:yilungmo@central.uh.edu) (Y.L. Mo).<https://doi.org/10.1016/j.tws.2017.10.038>

Received 22 August 2017; Received in revised form 12 October 2017; Accepted 17 October 2017

0263-8231/ © 2018 Elsevier Ltd. All rights reserved.

performed a few experimental and numerical researches on the elastic torsional behavior of BGCSWs under pure torsion and combined actions. Uehira et al. [28] considered the bending, shear and torsion separately and proposed the correction factors for the shear stresses in concrete slabs and CSWs and for the shear deformation of BGCSW through numerous case studies by finite element analysis (FEA). Meanwhile, he conducted a parametric study investigating the effect of diaphragm density on the torsional rigidity and the warping stresses [29]. After that, Li [30] conducted the experimental and numerical studies on the influence of multiple CSWs on the elastic torsional behavior of BGCSWs. In the actual design, however, the ultimate torsional capacity is now what the designers truly care about. Fortunately, a few investigators have focused their attentions on the torsional capacity of BGCSWs under pure torsion or combined actions. Mo et al. [31] first performed the reversed cyclic torsional tests with four reduced-scale specimens of single-cell BGCSWs with various compressive strengths of concrete and prestresses. Based on these specimens, Ding et al. [32] carried out a parametric study considering the influence of compressive strength of concrete and the shear modulus and thickness of CSWs on the torsional capacity. Then they tested four specimens subjected to pure torsion [33] and two specimens under the combined actions of torsion and bending [34]. In their tests, the effects of the thickness of CSWs and the shape parameter on the torsional behavior were considered. In addition, the influence of the bending moment on the torsional capacity was also discussed. Subsequently, Ko et al. [35] tested one specimen under pure torsion and provided four cases with different configurations of CSWs and thicknesses of concrete slabs by FEA to verify their proposed analytical model. Similarly, Dong et al. [36] carried out a pure torsional test with one specimen to validate the analytical and FEA models. To understand the difference between the BGCSWs with vertical and inclined CSWs, Wang [37] conducted the pure torsional tests with three specimens of BGCSWs to investigate the effect of the vertical inclined angles of CSWs on the ultimate torsional capacity. Moreover, he completed a parametric study which explored the crucial influence factors for the ultimate torques of BGCSWs, such as the compressive strength of concrete, the thickness of CSWs and the ratio of reinforcement.

From above research review, it can be concluded that the current experimental and numerical researches on the torsional behavior of BGCSWs either focused on the elastic torsional behavior or just concentrated on the full torsional behavior of single-cell BGCSWs. The full torsional behavior of multi-cell BGCSWs under pure torsion has not been investigated so far. To supplement the insufficiency of current study, two specimens of multi-cell BGCSWs are tested under pure torsion and the torsional responses in the whole loading process are obtained, including the torque-twist curves, the failure modes and the shear strains in concrete slabs and CSWs. Then the FEA models based on test specimens are verified by the experimental results and a parametric study is performed to better understand the detailed influence factors of torsional capacity. In addition, the torque-twist behavior of various multi-cell BGCSWs are predicted by FEA. The distribution of the shear strains in concrete slabs and CSWs are described in detail.

## 2. Experimental analysis

### 2.1. Test specimens

In this study, the scaled model tests are conducted with two specimens. One of the specimens is a single-box double-cell concrete BGCSW, named as T-2C, the other is a single-box triple-cell prestressed concrete BGCSW, named as T-3C. The dimensions and configurations of the BGCSWs are shown in Fig. 1 and Fig. 2. For the specimen of T-2C, the connections between CSWs and concrete slabs are the embedded shear connectors, i.e. both ends of the CSWs in the height direction are embedded into the concrete slabs, and the connections are strengthened by the transverse steel bars going through the holes of CSWs. For the

specimen of T-3C, the seven-wire, low-relaxation steel strands with a diameter of 15.2 mm are used as prestressed tendons, and the studs between CSWs and concrete slabs are arranged along the midlines of upper and lower steel flange plates at a spacing of 75 mm. The two basic connections are employed into the specimens to show the capability and applicability of the theory model in the companion paper [16]. In practice, they have been applied in bridges, such as Pohe Bridge [38] and Changzheng Bridge [39]. The other types of connections transformed from these two basic types have also been applied in other newly built box-girder bridges with CSWs, which will not be discussed herein. Solid end diaphragms with thicknesses of 0.2 m and 0.4 m for T-2C and T-3C, respectively, are attached at both ends of the specimens to provide space for the loading and fixed constraints. The material properties of the two BGCSWs are shown in Table 1.

### 2.2. Test setup and loading procedures

A new apparatus is designed and used in the tests, as shown in Fig. 3. One end of the test specimen is fixed by rigid steel beams as a fixed end and the other end is clamped by rigid steel beams as a rotating end. Both ends of the test specimen are held by the steel supports fixed on the strong floor. The pure torque is applied by a hydraulic servo control jack through the eccentric loading of rigid steel beam with a lever arm of 1.65 m. The bottom of the jack is fixed below the cross beam of load frame. A rotating hinge, several rollers and a pair of steel plates are assembled among the jack, load beam and load frame to avoid the inclining of jack. The rotating end can rotate freely around the rotating hinge. The roller bearings are placed between the rigid steel beams and the specimen at the rotating end to release the longitudinal constraint of specimen.

As shown in Fig. 3(e), the specimen is twisted around the rotating hinge under the rotating end, which will result in that the torsional center is not at the center of cross section of the specimen. It should be admitted that this shortage will lead to a few transverse offset at the rotating end. Fortunately, this shortage will not have a significant effect on the loading mode of pure torsion. The applied torque  $T$  can be obtained as

$$T = F'l' = \frac{F}{\cos \theta'} \left( \frac{l_1}{\cos \theta'} - l_2 \tan \theta' \right) = \frac{Fl_1}{\cos^2 \theta'} \left( 1 - \frac{l_2}{l_1} \sin \theta' \right) = Fl_1 \eta \quad (1)$$

where  $F'$  and  $l'$  are the resultant load applied on the load beam and the length of corresponding lever arm (BE), respectively;  $F$  and  $l_1$  are the load obtained from the load cell and the length of corresponding lever arm (BC), respectively;  $l_2$  is the initial height difference between the two rotating hinges;  $\theta'$  is the inclined angle of load beam respect to horizontal line (initial position);  $\eta$  is the correction coefficient,  $\eta = [1 - (l_2/l_1)\sin\theta'] / \cos^2\theta'$ . When the peak torque is reached, the inclined angle  $\theta'$  is small and  $\eta$  is close to 1, (i.e. when  $\theta' < 10^\circ$ ,  $0.967 < \eta < 1$ ), the applied torque can be approximately calculated as  $Fl_1$ .

As shown in Figs. 4 and 5, the strain gauges are attached on the surfaces of concrete slabs and CSWs, respectively, to monitor the resulting shear strains of specimens. In this study, the twists of the BGCSWs are assumed to be represented by the twists of concrete slabs. To assure the accuracy of the measured twists, several displacement meters (DMs) and inclinometers (IMs) are assembled on the lower surfaces of bottom concrete slabs and upper surfaces of top slabs, respectively, and the twists of specimens can be simultaneously obtained as

$$\theta_{DM} = \frac{1}{2} \left[ \frac{(\delta_{DM-1} + \delta_{DM-4})}{W_{DM-T}} - \frac{(\delta_{DM-5} + \delta_{DM-8})}{W_{DM-T}} + \frac{(\delta_{DM-2} + \delta_{DM-3})}{W_{DM-B}} - \frac{(\delta_{DM-6} + \delta_{DM-7})}{W_{DM-B}} \right] \quad (2)$$

Download English Version:

<https://daneshyari.com/en/article/6777661>

Download Persian Version:

<https://daneshyari.com/article/6777661>

[Daneshyari.com](https://daneshyari.com)